ARL-TR-7468 ● SEP 2015

US Army Research Laboratory

Numerical Computation of the Radar Cross Section of Rockets and Artillery Rounds

by Christopher Kenyon and Traian Dogaru

NOTICES

Disclaimers

The findings in this report are not to be construed as an official Department of the Army position unless so designated by other authorized documents.

Citation of manufacturer's or trade names does not constitute an official endorsement or approval of the use thereof.

Destroy this report when it is no longer needed. Do not return it to the originator.

ARL-TR-7468 ● SEP 2015

US Army Research Laboratory

Numerical Computation of the Radar Cross Section of Rockets and Artillery Rounds

by Christopher Kenyon and Traian Dogaru
Sensors and Electron Devices Directorate, ARL

REPORT DOCUMENTATION PAGE

Form Approved
OMB No. 0704-0188

1. REPORT DATE *(DD-MM-YYYY)*	2. REPORT TYPE	3. DATES COVERED (From - To)
Sep 2015	Final	Oct 2014–Aug 2015

4. TITLE AND SUBTITLE
Numerical Computation of the Radar Cross Section of Rockets and Artillery Rounds

5a. CONTRACT NUMBER

5b. GRANT NUMBER

5c. PROGRAM ELEMENT NUMBER

6. AUTHOR(S)
Christopher Kenyon and Traian Dogaru

5d. PROJECT NUMBER
R.0014706.20

5e. TASK NUMBER

5f. WORK UNIT NUMBER

7. PERFORMING ORGANIZATION NAME(S) AND ADDRESS(ES)
US Army Research Laboratory
ATTN: RDRL-SER-U
2800 Power Mill Road
Adelphi, MD 20783-1138

8. PERFORMING ORGANIZATION REPORT NUMBER
ARL-TR-7468

9. SPONSORING/MONITORING AGENCY NAME(S) AND ADDRESS(ES)

10. SPONSOR/MONITOR'S ACRONYM(S)

11. SPONSOR/MONITOR'S REPORT NUMBER(S)

12. DISTRIBUTION/AVAILABILITY STATEMENT
Approved for public release; distribution unlimited.

13. SUPPLEMENTARY NOTES

14. ABSTRACT
This report investigates the modeling of radar scattering from rocket, artillery, and mortar (RAM) targets in 4 radar frequency bands: L, S, C, and X. Three targets are selected for this study: a 155-mm artillery round, and a 107-mm rocket, with and without stabilization fins. The radar cross section (RCS) calculations are performed by 2 different methods, implemented by the FEKO and AFDTD electromagnetic simulation software packages, over all the possible aspect angles. The solutions obtained by the 2 methods are compared for accuracy validation. The RCS analysis includes prediction of the variation with frequency and the azimuth angle (for non-symmetric targets), as well as a comparison among the 4 frequency bands of interest. The target signature calculations in this study are an important tool for radar engineers in system performance evaluation.

15. SUBJECT TERMS
Computational electromagnetics, radar signature

16. SECURITY CLASSIFICATION OF:			17. LIMITATION OF ABSTRACT	18. NUMBER OF PAGES	19a. NAME OF RESPONSIBLE PERSON
a. REPORT	b. ABSTRACT	c. THIS PAGE			Traian Dogaru
Unclassified	Unclassified	Unclassified	UU	32	19b. TELEPHONE NUMBER (Include area code) (301) 394-1482

Contents

List of Figures

List of Tables

INTENTIONALLY LEFT BLANK.

1. Introduction

The US Army is interested in the radar detection and tracking of artillery rounds grouped under the generic category of rockets, artillery, and mortar (RAM). Two obvious applications of this type of radar are counter-fire measures and active protection against projectiles. One important step in the radar system design consists of analyzing the radar cross section (RCS) of the targets of interest. The electromagnetic (EM) modeling team at the US Army Research Laboratory (ARL) has developed capabilities for modeling the radar signature of a wide variety of targets, using multiple numerical EM simulation methods. In this report, we apply 2 of these EM software packages, AFDTD and FEKO, to the RCS calculation of some typical RAM targets.

More specifically, the set of targets of interest for this investigation includes rocket artillery rounds (with ranges under 100 km) and gun artillery rounds. A follow-up report will analyze the RCS of mortar rounds. For our analysis, we picked a 107-mm rocket, with and without stabilization fins, and a 155-mm artillery round. The computational meshes, presented in Section 2, were built in-house from drawings available on public websites and do not necessarily contain all the construction details (such as the rocket exhaust nozzles). Nevertheless, the analysis includes all the features relevant to our phenomenological study.

The goals of this report are the following:

- Evaluate the RCS of the targets of interest in the L, S, C, and X radar bands and compare their magnitudes across the bands. In all cases, the RCS is computed with respect to the aspect angle, with the target placed in a standard (upright) orientation.
- Assess the accuracy of the simulations by AFDTD and FEKO for these targets in the frequency bands of interest. Notice that, although the target geometry and environment seem relatively simple compared to some of our previous modeling work, the radar scattering phenomenology from these targets presents some subtle effects (surface wave phenomena in particular) that make the accurate RCS calculations rather challenging.
- Quantify the variation of the target RCS for small frequency deviations within the radar bands already mentioned. This analysis is useful for a radar system that uses frequency agility.
- Study the variation of the target RCS with the azimuth angle for targets that cannot be described as rotationally symmetric. This is the case of the rocket with fins.

A follow-up investigation will analyze the RCS variations of in-flight RAM targets, as measured by the ground-based stationary radar system.

Previous work performed in this area has not been systematically documented and is generally not available in the public domain. Several Army databases catalogue the RCS of some RAM-type targets in certain frequency bands; however, the documentation does not always specify the RCS evaluation method (measurement or simulation). Otero et al.[1] contains a useful analysis of RAM target RCS, including its variations for in-flight projectiles. That report lists several numerical modeling codes for RCS calculation, but does not state clearly which code was used in the specific examples analyzed there. This is an important issue, since, as previously mentioned, only advanced, full-wave EM modeling techniques produce accurate results for these types of simulations, whereas approximate legacy codes (such as those based on ray-tracing) are known to handle certain essential radar scattering phenomenological aspects with less accuracy.

This report is organized as follows. In Section 2, we present the targets under investigations and the numerical methods used in computing the radar signature. Section 3 compares the accuracy of the 2 EM modeling software packages employed in this work and takes a closer look at some specific modeling issues. In Section 4 we analyze the variations of the RCS with frequency, within and across the 4 frequency bands of interest. For projectiles which do not exhibit rotational symmetry, we look at their RCS variation with azimuth aspect angle in Section 5. We end with conclusions in Section 6.

2. Description of Radar Targets and Computational Methods

The radar targets under investigation in this report are shown in Fig. 1. For a conventional gun artillery round, we chose a 155-mm projectile (Fig. 1a), which is one of the most frequently encountered calibers for this type of munition. It is used by the armed forces of many countries, and some of its modern versions have reached a high degree of technological sophistication (such as the US-made, global positioning system [GPS]-guided Excalibur munition).

In terms of artillery rockets, we chose a 107-mm rocket. The version without stabilization fins (shown in Fig. 1b) has a fairly simple geometry – the only complex detail consists of the detonation tip that looks like a stack of several cylinders of receding diameters. Fig. 1c shows a version of the same rocket that includes the stabilization fins. The purpose of performing separate simulations on the 2 types of rockets is to assess the impact of the fins on the target RCS, as well as understand the signature variations of rotationally asymmetric targets when the azimuth angle changes. Notice that fin-stabilized rockets fired from typical rocket launcher

systems are usually equipped with foldable fins that are slightly curved (to conform to the rocket's cylindrical body surface). Since the curved fin geometry was too complicated to model with our available tools, we opted for straight fins, as shown in Fig. 1c.

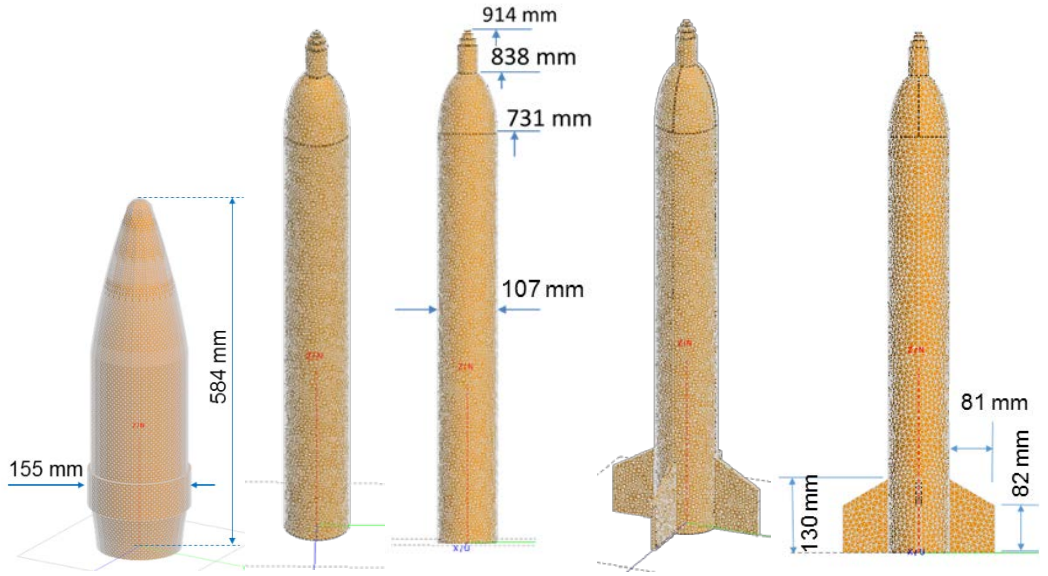

Fig. 1 Representation of the target meshes considered in this study, showing the most relevant physical dimensions: a) 155-mm artillery round, b) 107-mm rocket without stabilization fins, and c) 107-mm rocket with stabilization fins

Two different EM modeling programs were used in this study: FEKO and AFDTD. FEKO[2] is a commercial software package that includes several methods of solving general EM wave propagation problems, including radar scattering. In this work, we used the surface integral equation (SIE) solver (also known as the Method of Moment) for the RCS calculation of the targets of interest. AFDTD[3] is an EM modeling software package developed in-house at ARL specifically for radar signature simulations. It is based on the finite-difference time-domain (FDTD) method[4] and has been employed and validated in many radar system modeling applications of interest to the Army.

The primary purpose for using 2 full-wave simulation methods for the RCS calculation is to assess their accuracy. Nevertheless, an additional goal is to understand other program capabilities, such as efficiency, flexibility, availability, and limitations to the model sizes or frequency bands that can be handled. Besides the differences in the EM modeling algorithms implemented by the 2 software packages, we had to take into account the platforms and type of licenses available to the investigators. Thus, FEKO was used under a shared license agreement on

desktop personal computers (PC) running Windows, using a maximum of 4 cores at a time and with a memory limit of 96 GB. On the other hand, AFDTD, which was developed and is maintained by ARL employees, is a fully parallelized code that runs on multiple high-performance computing (HPC) platforms at the Defense Supercomputing Resource Centers (DSRCs). These features make the code available at any time and practically remove the memory and number of cores limitations inherent to the FEKO Windows-based commercial license.

For this investigation, the AFDTD code was run on the following platforms: Excalibur (Cray XC40) at the ARL DSRC,[5] Lightning (Cray XC30) at the Air Force Research Laboratory DSRC,[6] and Shepard (Cray XC30) at the Navy DSRC.[7] The number of cores used in each simulation varied from 4 (in the case of the 155-mm round) to 24 (in the case of the 107-mm rocket with fins).

In all the models presented in this work, the targets are made of perfect electric conductor (PEC) and are placed in free-space in the upright position (as shown in Fig. 1, where the *z* and projectile axes coincide). The simulation results are typically presented as RCS in decibel-square-meter (dBsm) versus elevation angle θ (measured from the *z* axis). The elevation angle varies between 0° and 90° in 0.5° increments. Both vertical-vertical (V-V) and horizontal-horizontal (H-H) polarizations are considered. The calculations are performed at 4 specific frequencies: 1.3 GHz (corresponding to the L band), 2.4 GHz (corresponding to the S band), 5.6 GHz (corresponding to the C band), and 9.5 GHz (corresponding to the X band). In the case of the 107-mm rocket with fins, we also vary the azimuth angle between 0° and 45°, in 5° increments.

One clear advantage of using the AFDTD program when different frequency bands are involved is that the calculations can be performed in 1 run for all bands (for 1 set of aspect angles). Moreover, this software makes it possible to save the modeling data at any in-between frequency points within a certain interval, which allows us to quantify the RCS variations encountered by a radar using frequency agility.[8] In all the AFDTD simulations presented in this report, we used an 4th order Rayleigh impulse[9] excitation, with a peak frequency of 3.35 GHz – this choice allowed the coverage of the entire frequency range of interest (from 1.2 to 9.6 GHz) for the output data.

The computational meshes were first created in the computer-aided design (CAD) module of the FEKO software (CAD FEKO) and then converted to AFDTD-compatible meshes by the AFDTDGRID program.[10] The 2 types of meshes are very different in nature: the FEKO mesh for the SIE solver consists of a description of the target surface using triangular patches, whereas the AFDTD mesh is a volumetric grid made of small cubic cells. There are certain requirements for the

patch or cell size in order to obtain an accurate solution at a given frequency. Thus, the usual rule of thumb dictates the size of these geometric elements be about $\lambda/10$,[11] where λ is the wavelength of the radar waves. However, when setting the spatial discretization element size, other considerations, such as available computational resources or the need to describe fine geometrical target features, may override these requirements.

In the case of FEKO, the user has some qualitative choices for the surface element average size (fine, standard, coarse). In our models, we chose the "standard" element size for the L and S bands, and the "coarse" size for the C and X bands. The latter choice was dictated by limits in the computer platform memory size. In quantitative terms, the average element size for the "standard" option is about 1 cm (or roughly $\lambda/12$ at S band), while for the "coarse" option it is about 0.4 cm (or roughly $\lambda/8$ at X band). The good match between the FEKO and AFDTD results (presented in Section 3) indicate that there was no loss of accuracy due to choosing the "coarse" mesh option for the higher frequency bands.

For the AFDTD simulations, we found that a cell size of 1 mm is necessary in order to obtain accurate results (this point is illustrated in Section 3 where we compare the solutions obtained on grids with 1- and 2-mm resolution, respectively). Notice that this cell size is significantly smaller than the $\lambda/10$ requirement, even at X band (in the context of FDTD algorithms, this spatial sampling rate limit is dictated by the need to keep the numerical dispersion under control).[4] However, since the boundaries of targets non-conformal to the main Cartesian planes are always subject to the staircasing errors of the volumetric discretization scheme, higher spatial sampling rates may be necessary to capture all the relevant details of the target geometry. The simulation examples in this study confirm this to be the case, at least for the 155-mm artillery round.

A direct comparison of the efficiency of the 2 EM modeling programs is difficult to perform, since they are based on different underlying algorithms, operate with different strategies to obtain RCS data over multiple frequencies and aspect angle, and run on different platforms in terms of central processing unit (CPU) speeds, memory sizes, and parallel processing capabilities. For instance, to obtain the RCS of the 107-mm rocket over the angular range mentioned previously, in all frequency bands, and for both polarizations, FEKO would require about 300 CPU hours, whereas AFDTD would require about 2000 CPU hours. However, in terms of wall-clock runtime, the parallel AFDTD runs can be completed in less than an hour (subject to the shared HPC platform current workload), whereas the FEKO runs may take more than a day to complete.

3. Comparison of FEKO and AFDTD RCS Predictions

In this section, we present the results of the AFDTD and FEKO simulations for the set of targets introduced in Section 2. Each graph in Figs. 2 through 4 represents the RCS versus elevation angle, and each subfigure plots together the AFDTD and FEKO results for V-V and H-H polarizations, for 1 frequency band. In the case of the 107-mm rocket with stabilization fins, we show the RCS results for azimuth angles of 0° and 30°. Notice that, for this target, only the results in the L, S, and C bands were available at the report publication time.

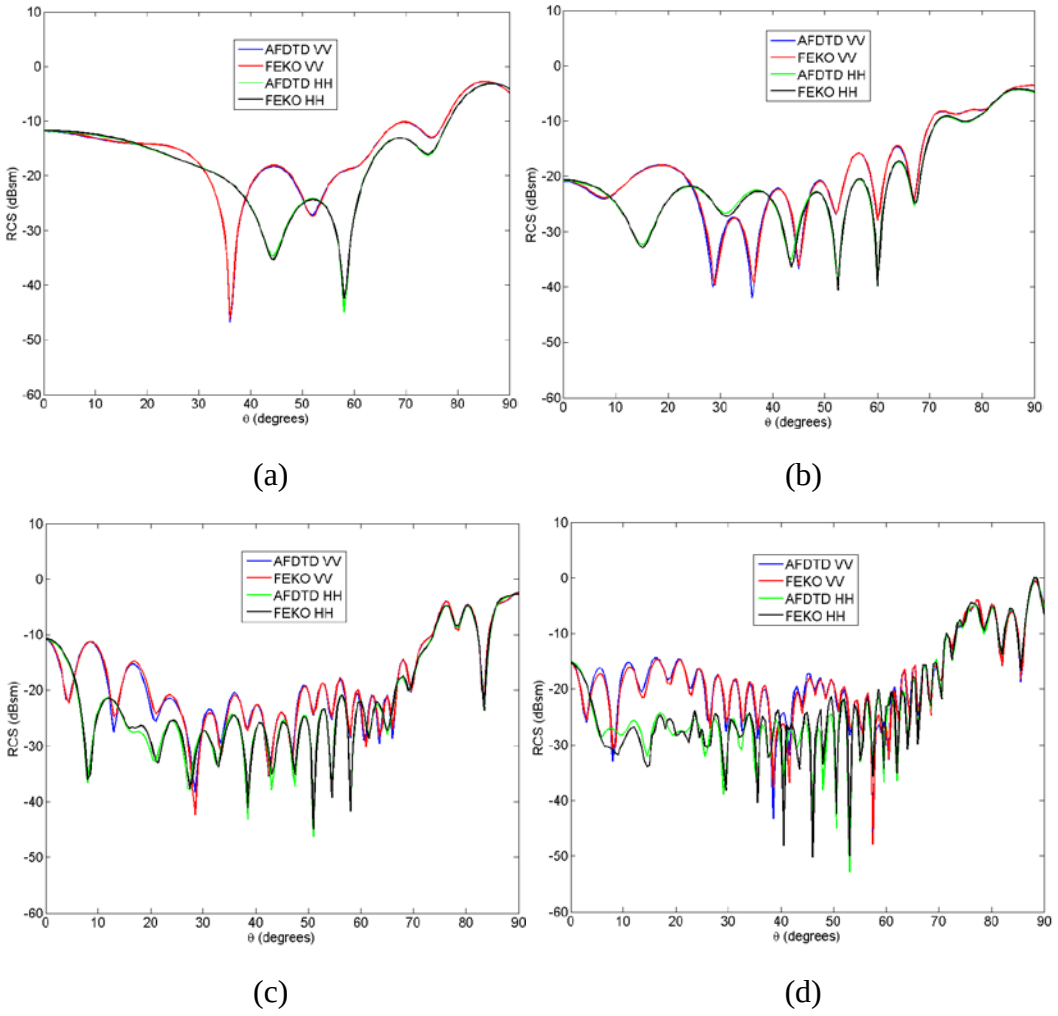

Fig. 2 RCS of the 155-mm artillery round vs. elevation angles, computed by the AFDTD and FEKO software in 4 radar frequency bands: a) L-band, b) S-band, c) C-band, and d) X-band

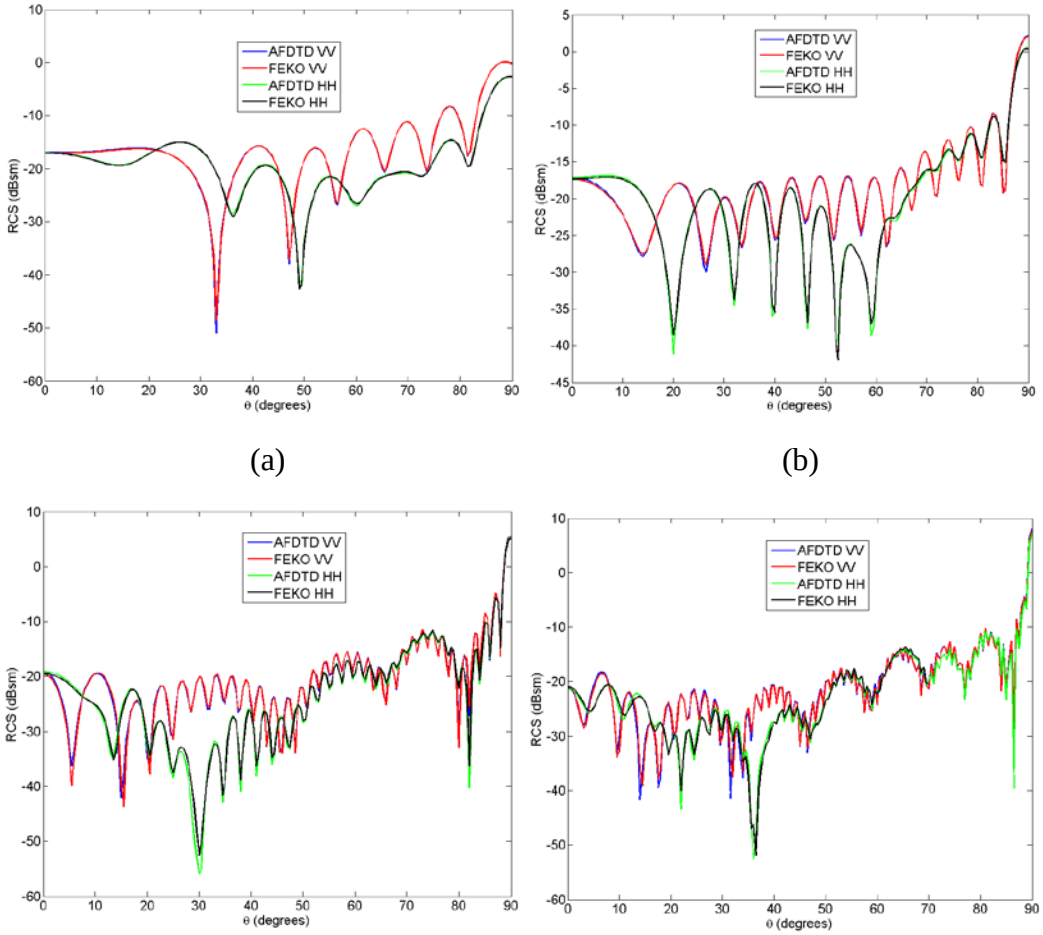

Fig. 3 RCS of the 107-mm rocket without stabilization fins vs. elevation angles, computed by the AFDTD and FEKO software in 4 radar frequency bands: a) L-band, b) S-band, c) C-band, and d) X-band

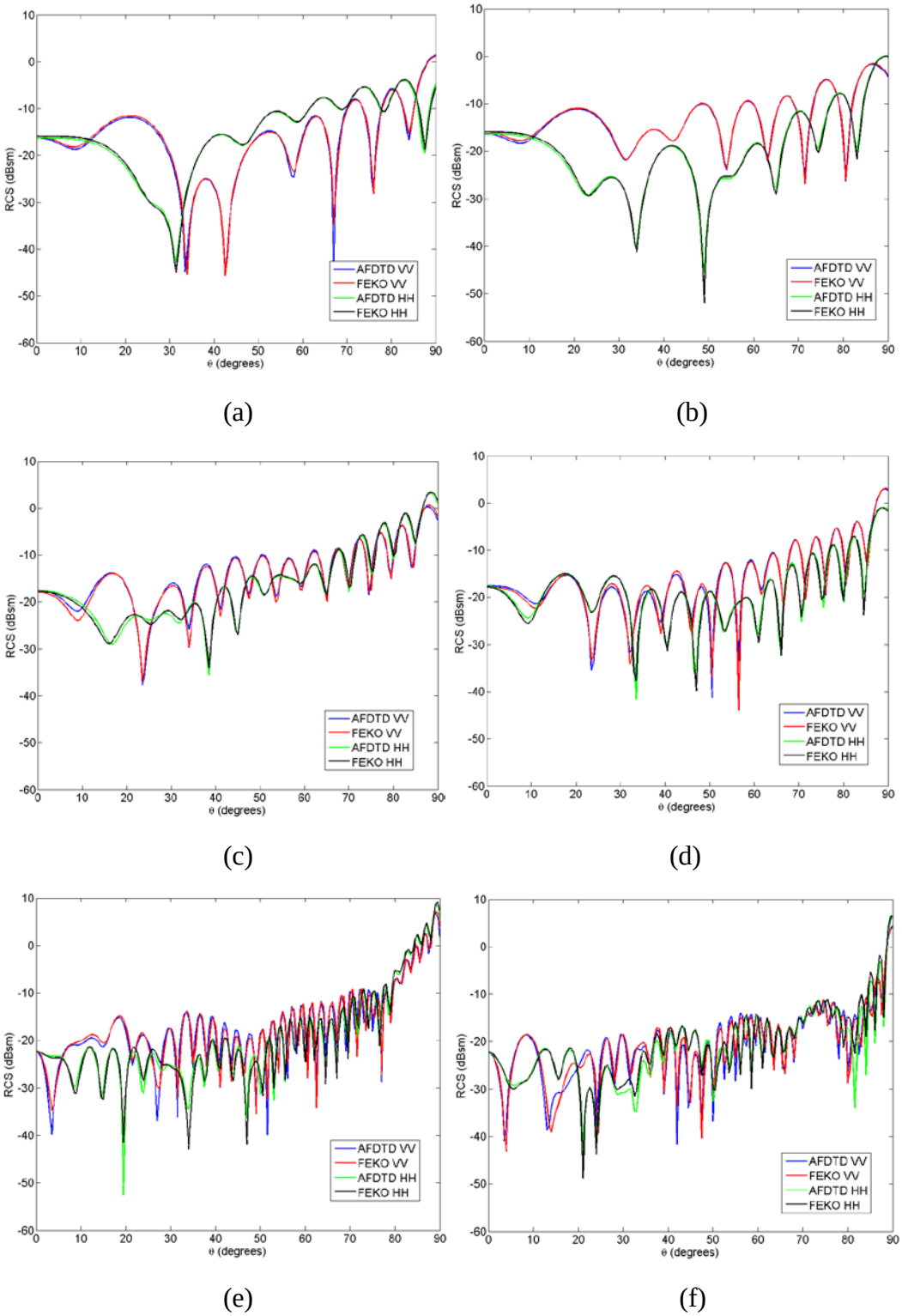

Fig. 4 RCS of the 107-mm rocket with stabilization fins vs. elevation angles, computed by the AFDTD and FEKO software in 4 frequency bands: a) L-band, ϕ = 0°; b) L-band, ϕ = 30°; c) S-band, ϕ = 0°; d) S-band, ϕ =30°; e) C-band, ϕ = 0°; and f) C-band, ϕ = 30°

There are only a few comments to make regarding the results in Figs. 2–4. First, we note the remarkable match between the AFDTD and FEKO solutions, which stays within 2 dB most of the time (except for some nulls of the graphs, where matching various simulation results is always extremely challenging). As expected, the mismatch is slightly higher in the C and X bands, where both modeling methods are expected to lose some accuracy. The RCS characteristics of the projectiles exhibit faster angular variations as the frequency increases. At the same time, the RCS generally increases with the elevation angle (as the aspect changes from nose-on view to side view), which is the expected result given the geometry of these targets. In terms of polarization, we notice that, on the average, there are no major differences between the RCS for V-V and H-H modes. Although at low-to-mid-range angles, the V-V RCS seems to have higher values than the H-H RCS; the 2 polarizations tend to merge when the aspect angle approaches broadside – this effect is more clearly visible in the higher frequency bands (C and X).

One interesting phenomenological aspect about the radar scattering from long and thin metallic targets is the importance of surface waves to the overall signature.[12] These waves propagate along the surface of the object and incur successive reflections at the 2 ends. While present for V-V polarization at any incidence angle, they form the dominant contribution to the backscattering response only for close-to-nose-on viewing angles. The surface waves must be treated with particular care in any FDTD-based simulation (which operates in the time domain), by choosing a runtime long enough to insure that the target end reflection contributions decay to a negligible level before the simulation is stopped. To illustrate this point, in Fig. 5a, we show the range profile of the 107-mm rocket obtained with AFDTD after 5536 and 16000 time steps, respectively (the time step interval is 1.67 ps), at $\theta = 0°$. Notice that, if we truncate the run after only 5536 time steps, we miss the second round-trip reflection of the surface wave (third peak in the range profile), which has a significant contribution to the signature. On the other hand, subsequent surface wave contributions (at ranges of 2 m and beyond) are below the noise level and can be neglected. Figure 5b shows the impact of the early runtime truncation error on the RCS calculation, by comparing the truncated solution (5536 time steps) with the correct one (obtained after 16000 time steps). As expected, the differences are visible only for angles θ up to about 45°, beyond which the surface wave contribution to the signature becomes negligible.

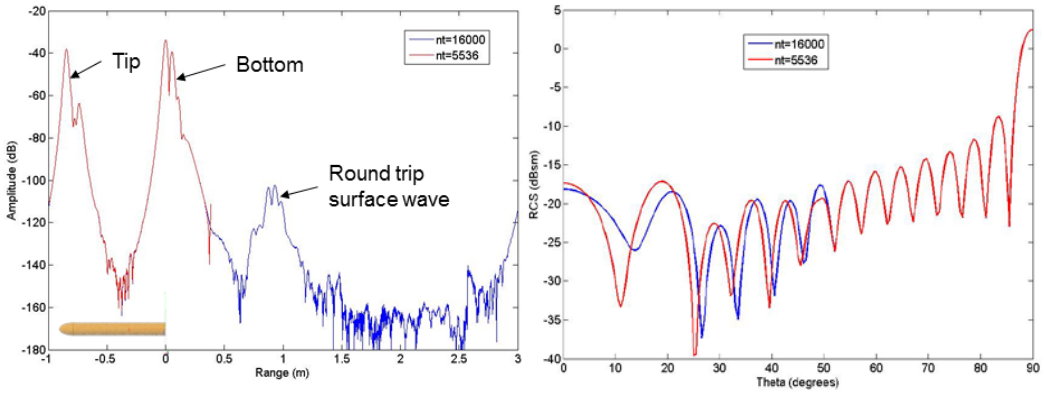

(a) (b)

Fig. 5 Illustration of the errors in modeling surface waves by AFDTD, for the 107-mm rocket. a) Range profile at $\theta = 0°$ and b) RCS vs. θ at S-band, V-V polarization.

The plots in Fig. 6 support the choice of a 1-mm resolution grid in the AFDTD models, by comparing the RCS of the 155-mm round obtained on a 1-mm grid (already validated against FEKO) and 2-mm grid. The results in this figure clearly show significant differences between the 2 solutions in the X bands, demonstrating that the 2-mm grid resolution is not satisfactory for this analysis (notice that, although not shown here, the errors are smaller in the L, S and C bands).

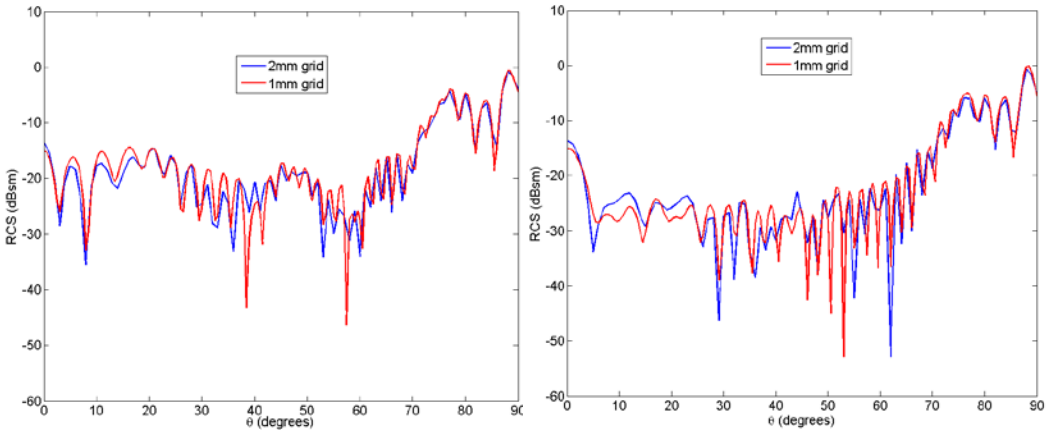

(a) (b)

Fig. 6 RCS of the 155-mm artillery round computed by AFDTD in the X-band, using grids with 1- and 2-mm resolution, respectively, showing a) V-V polarization; and b) H-H polarization

4. Variation of RCS with Frequency

The next step in our analysis is to study the RCS variation with frequency for the targets of interest. One aspect of this analysis is concerned with the RCS variation

of the targets within each frequency band considered here. The other part of the analysis consists of comparing the radar signatures among the 4 frequency bands. All the results in this section were obtained with the AFDTD software.

Although the radar systems that detect and track artillery projectiles transmit signals with very narrow bands, the center frequencies of these signals may change in time (not necessarily pulse-to-pulse), sometimes in a random manner – this feature of a radar system is called frequency agility. Therefore, it is interesting to see how much the target signature changes within a relatively wider frequency range, even as we nominally stay within the limits of the same frequency band. For our analysis, we computed the RCS of the targets of interest over a bandwidth of 200 MHz, centered at each of the 4 frequencies listed in Section 2. Thus, for the L band we considered frequencies between 1.2 and 1.4 GHz; for the S band, between 2.3 and 2.5 GHz; for the C band, between 5.5 and 5.7 GHz; and for the X band, between 9.4 and 9.6 GHz. Within each of these bands, we computed the RCS at 50-MHz intervals.

The graphs in Figs. 7 through 9 illustrate the variation of the RCS within each frequency band as error bar plots. Namely, the continuous blue line represents the average RCS at a given angle within the band, while the error bars show the upper and lower limit of the RCS within the same band. Additionally, the graphs represent the RCS at the middle frequencies of each band (red continuous line) – these are the same plots as those in Figs. 2–4. The conclusion one can draw from these graphs is that, generally, the RCS variation within a frequency band is relatively small (about 2 dB) when the baseline RCS value is large enough (over –10 dBsm for this set of targets), and becomes larger when the baseline RCS is small. (Keep in mind that the differences illustrated in these graphs are measured in dB, therefore they represent *ratios* of the various quantities.)

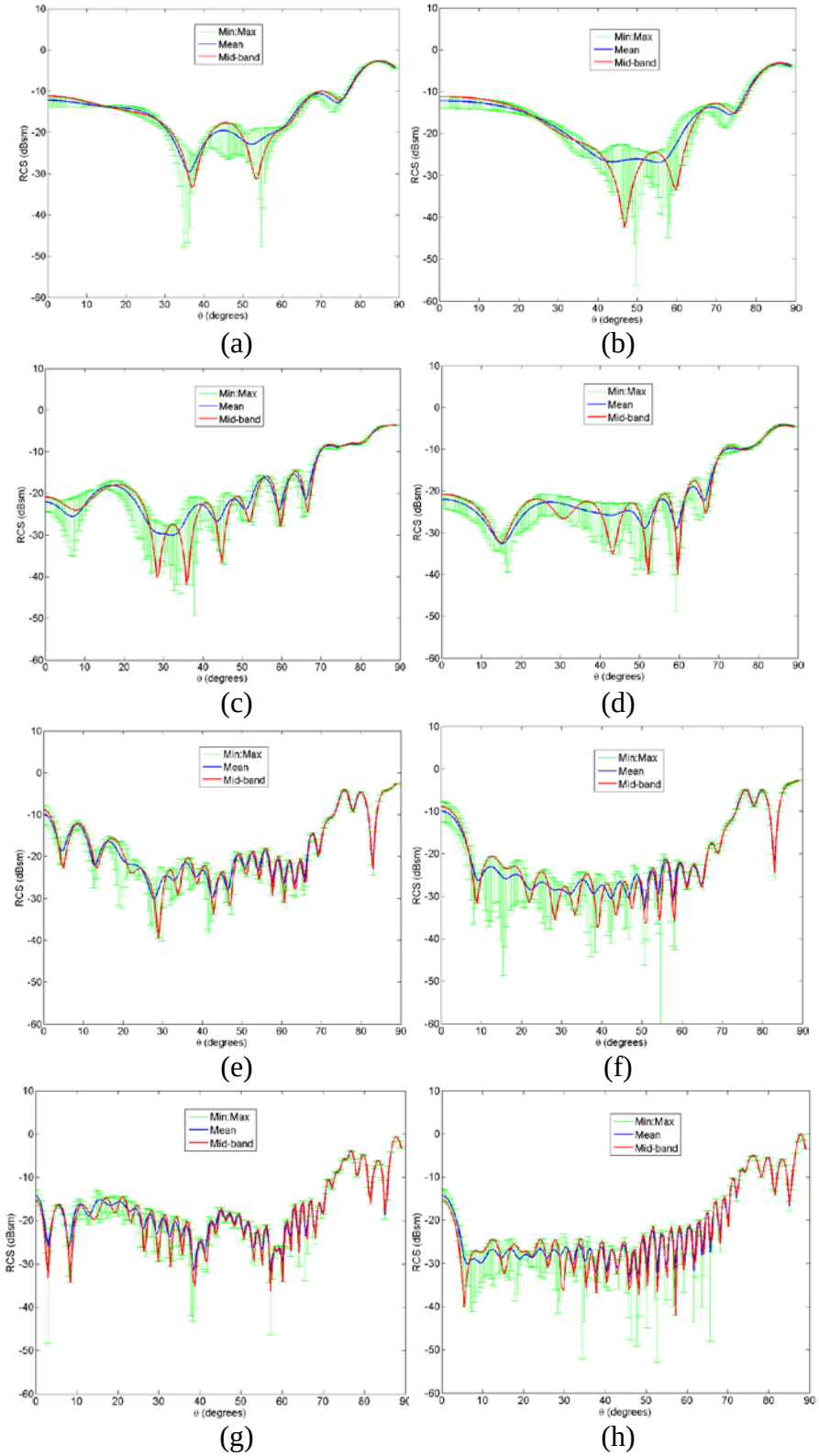

Fig. 7 Mean, mid-band, and upper-lower limit RCS of the 155-mm artillery round computed by AFDTD over a 200-MHz bandwidth, in all 4 radar frequency bands, for a) L-band, V-V; b) L-band, H-H; c) S-band, V-V; d) S-band, H-H; e) C-band, V-V; f) C-band, H-H; g) X-band, V-V; and h) X-band, H-H

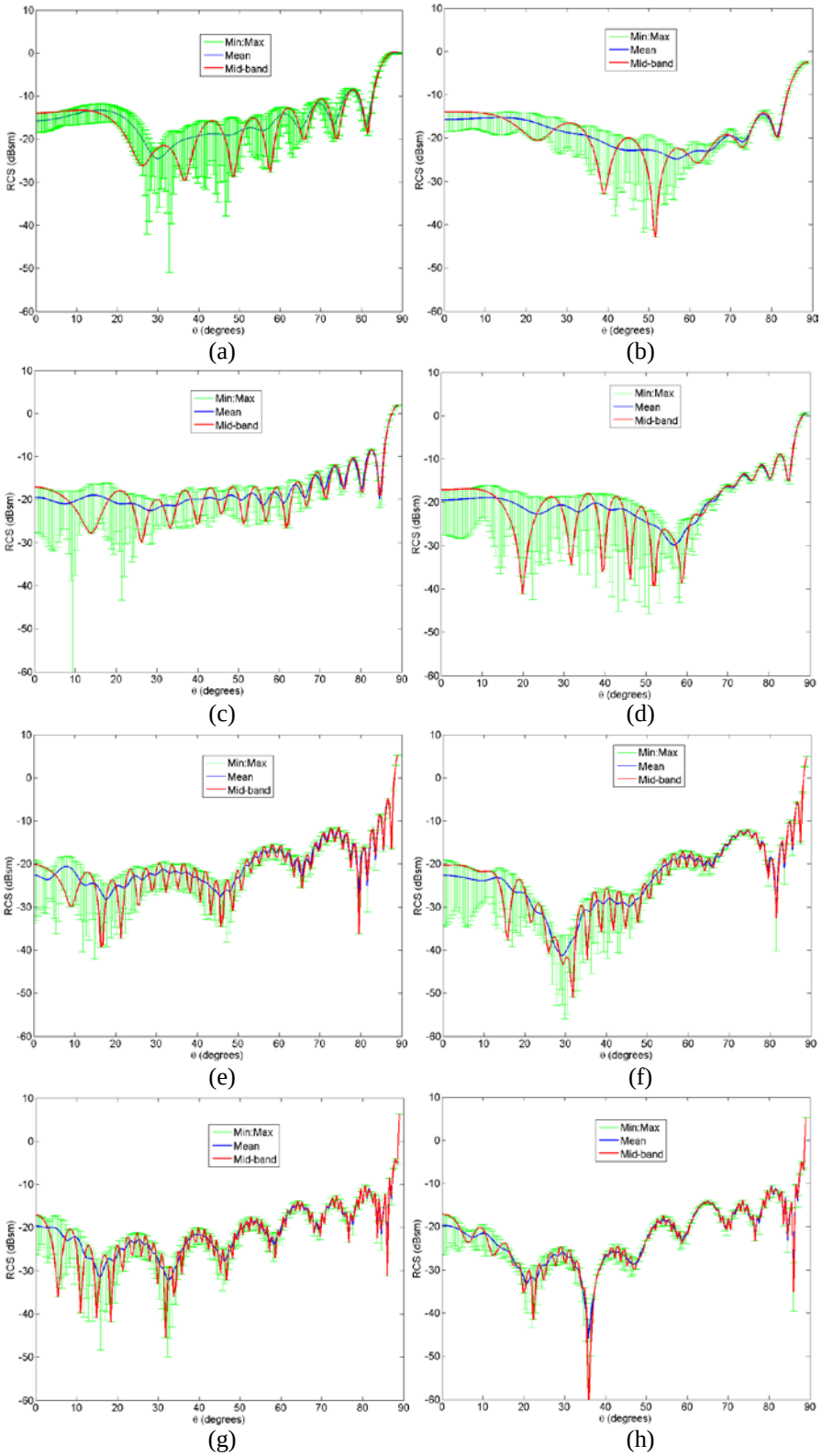

Fig. 8 Mean, mid-band, and upper-lower limit RCS of the 107-mm rocket without stabilization fins computed by AFDTD over a 200-MHz bandwidth, in all 4 radar frequency bands, for a) L-band, V-V; b) L-band, H-H; c) S-band, V-V; d) S-band, H-H; e) C-band, V-V; f) C-band, H-H; g) X-band, V-V; and h) X-band, H-H

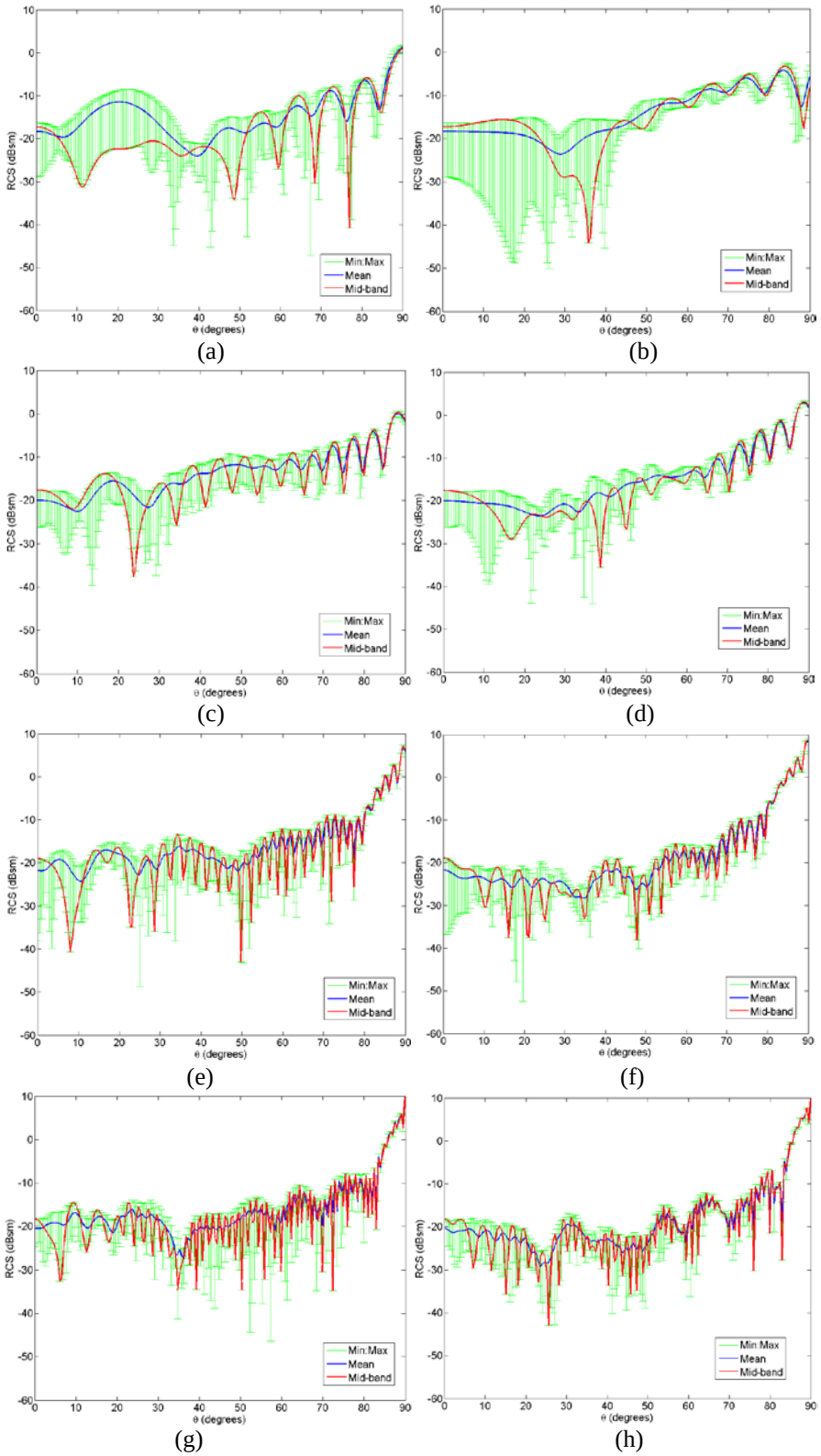

Fig. 9 Mean, mid-band, and upper-lower limit RCS of the 107-mm rocket with stabilization fins computed by AFDTD over a 200-MHz bandwidth, at $\phi = 0°$, in all 4 radar frequency bands, for a) L-band, V-V; b) L-band, H-H; c) S-band, V-V; d) S-band, H-H; e) C-band, V-V; f) C-band, H-H; g) X-band, V-V; and h) X-band, H-H

Figures 10 through 12 replot the RCS versus elevation angle characteristics obtained in Section 3 for the 3 targets, but this time groups the graphs for all 4 frequency bands together (for a given target and polarization). This offers an easy-to-read comparison of the RCS in the various bands. The RCS in each band is taken as the average over the 200-MHz frequency intervals specified in a previous paragraph of this section. Additionally, for the 107-mm rocket with fins, the RCS is averaged over the azimuth angles mentioned in Section 2. Table 1 contains the average RCS over all aspect angles (elevation and azimuth), taken with equal weights, for each case.

One thing to notice from these results is the remarkably tight range of each target average RCS (typically no more than 3 dB), irrespective of frequency band or polarization. The only target that exhibits slightly larger RCS values for the upper frequency bands (compare X-band with L-band) is the rocket with stabilization fins. One closer look at the plots in Fig. 12 reveals that most of these differences occur at elevation angle close to broadside, where the RCS increases much faster in the C- and X-band than at lower frequencies. The RCS increase with frequency for this target is characteristic to the backscattering from the corners formed by the rocket's fins, which appear to have a large contribution to the overall radar response at angles close to broadside.

Nevertheless, when discussing the choice of radar frequency band in the context of system performance, one should keep in mind that the RCS magnitude is only 1 factor determining the target detectability (via the radar equation),[8] and that many other system parameter considerations should be taken into account in choosing the optimum frequency band.

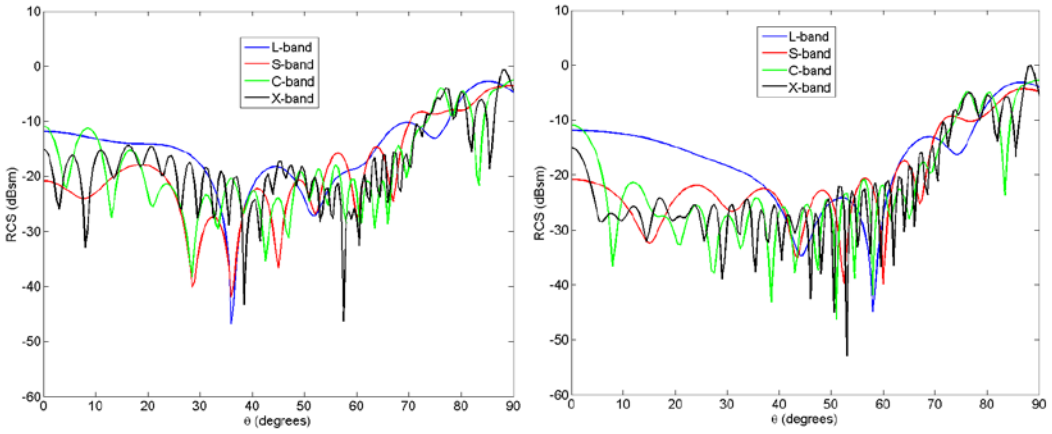

Fig. 10 Average RCS of the 155-mm artillery round computed by AFDTD in all 4 radar frequency bands, for a) V-V polarization; and b) H-H polarization

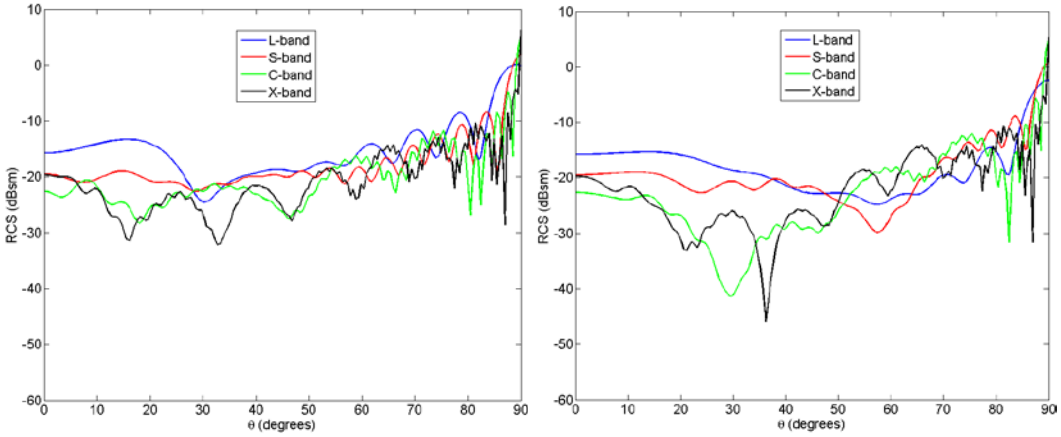

(a) (b)

Fig. 11 Average RCS of the 107-mm rocket without stabilization fins computed by AFDTD in all 4 radar frequency bands, for a) V-V polarization; and b) H-H polarization

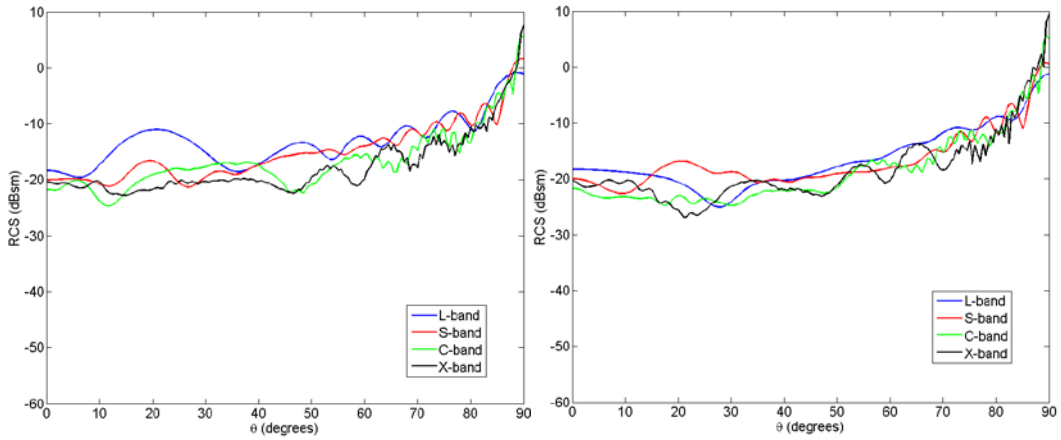

(a) (b)

Fig. 12 Average RCS of the 107-mm rocket with stabilization fins computed by AFDTD in all 4 radar frequency bands, for a) V-V polarization; and b) H-H polarization

Table 1 Mean RCS (in dBsm) of the 3 targets considered in this study, computed over all possible aspect angles and a 200-MHz bandwidth within each of the 4 frequency bands

Target	155-mm round		107-mm rocket (no fins)		107-mm rocket (with fins)	
Polarization	V-V	H-H	V-V	H-H	V-V	H-H
L-band	–10.91	–11.71	–11.04	–14.27	–10.20	–12.37
S-band	–12.36	–13.28	–12.66	–13.57	–10.60	–11.76
C-band	–12.18	–12.64	–13.06	–13.60	–10.10	–10.20
X-band	–12.11	–12.64	–13.76	–14.62	–9.89	–8.42

5. Variation of RCS with Azimuth Angle for Non-Symmetric Targets

If a target does not exhibit rotational symmetry, its radar signature depends on the azimuth angle. For the 107-mm rocket with 4 fins, we are interested in the variation of the RCS in an azimuth angular sector of 45° (every other 45° sector will contain the same RCS values). To study the variation of this target's signature with the azimuth aspect angle, we calculated its RCS versus elevation angle, in the middle of the L, S, C, and X bands, for $\phi = 0°$ to 45°, in 5° increments. The plots in Fig. 13 are similar to those in Figs. 7–9, with the difference that now the error bar spans the upper and lower RCS limits when the azimuth angles varies as indicated. This time, we notice sizeable magnitude swings in the signature, even for relatively large RCS values. One exception are the points close to noise-on incidence, where obviously the azimuth orientation does not play a role in determining the radar response.

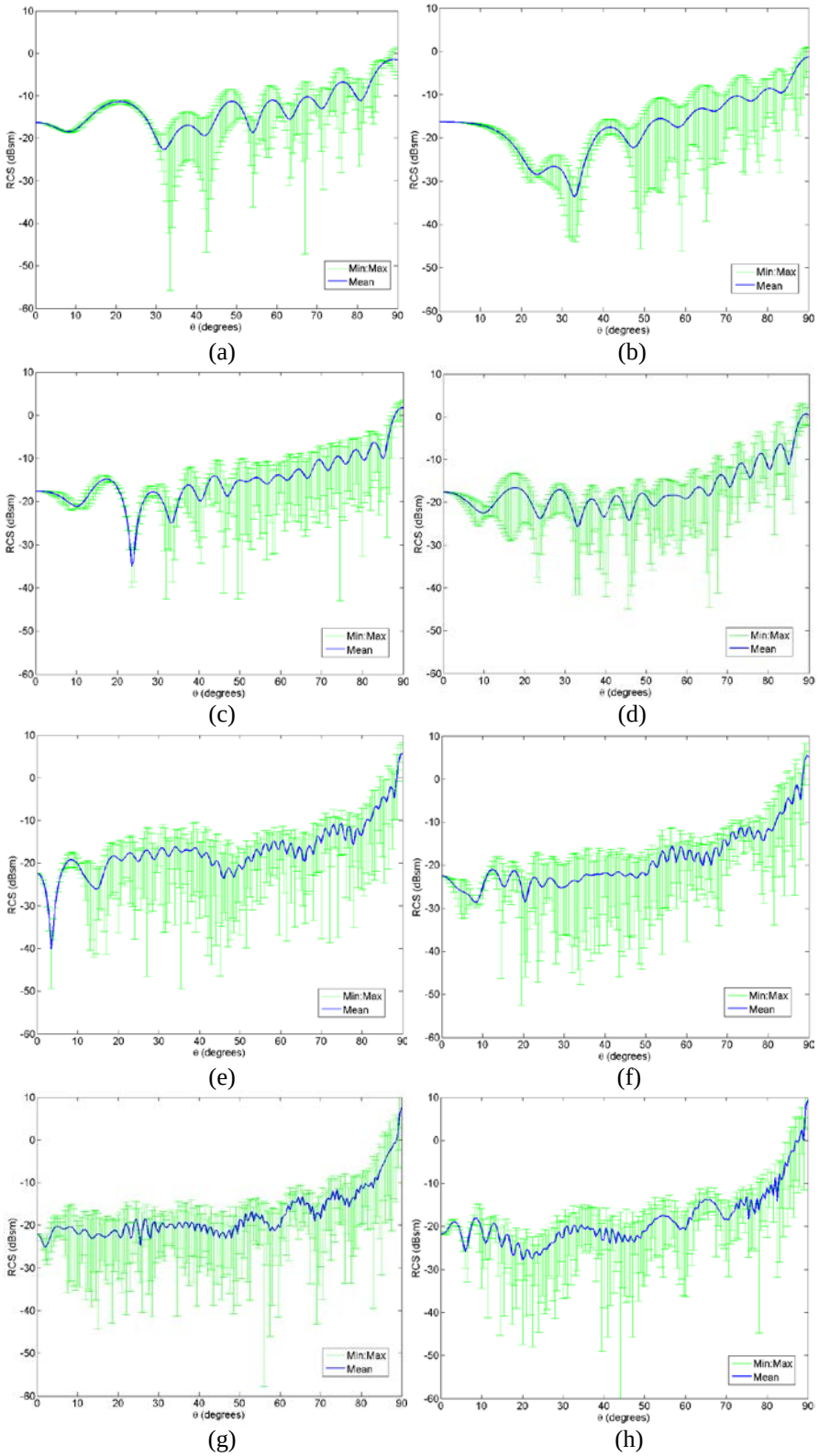

Fig. 13 Mean and upper-lower limit RCS of the 107-mm rocket with stabilization fins computed by AFDTD over a 45° azimuth angular range, in all 4 radar frequency bands, for a) L-band, V-V; b) L-band, H-H; c) S-band, V-V; d) S-band, H-H; e) C-band, V-V; f) C-band, H-H; g) X-band, V-V; and h) X-band, H-H

From a practical standpoint, the large variation in RCS for projectiles equipped with stabilization fins with respect to the azimuth aspect makes it difficult to predict their radar signature with reasonable accuracy in a real-life scenario. During the projectile flight, the azimuth orientation is completely random for a ground-based observer, so even if we have all the information on the ballistic trajectory, the RCS can only be predicted in a statistical manner, by indicating an average value and upper/lower limits of variation.

6. Conclusions

This report demonstrated the capabilities of our EM modeling tools to predict the RCS of typical RAM targets, such as the 155-mm artillery round and the 107-mm artillery rocket. The software program employed in this work were FEKO and AFDTD. Although the underlying modeling techniques are very different in the 2 codes, the results matched very well over all the frequencies and angles of interest.

Other findings of our investigation showed that, on average, there are no significant differences in the radar signature of these targets among the 4 frequency bands considered here (L, S, C, and X bands), as well as between V-V and H-H polarizations. Additionally, the RCS did not vary significantly within those bands, when we considered frequency deviations of ±100 MHz over the middle frequency. However, for rotationally non-symmetric targets (such as rockets with stabilization fins), we found significant variations in the RCS with the azimuth aspect angle.

Looking ahead, we are confident in recommending the AFDTD software for future studies of RAM target radar signatures. This method requires fine grid resolutions (down to a 1-mm cell size for frequencies as high as 10 GHz); however, the ability to run the AFDTD code on large, parallel HPC platforms should mitigate the large grid sizes resulting from the fine target discretization. Other advantages of this code in terms of efficiency, flexibility, and availability were discussed in Section 2.

One type of RAM targets that was left out of this report is the mortar round. Its radar signature will be investigated in a separate report, using both simulations methods (FEKO and AFDTD).

A follow-up study will look at predicting the RCS of in-flight RAM targets, using realistic ballistic trajectories. For this purpose, the coordinates and orientation of the projectile, as well as the radar coordinates will determine the radar-to-target aspect angle, while the results presented in this report will provide a look-up table for RCS values. By this procedure, we will be able to predict the RCS variation over time, allowing for eventual statistical variations that account for the unknown azimuth orientation of the in-flight projectile. Hopefully, these simulations will

provide a useful performance prediction tool to the radar engineers designing systems dedicated to detection and tracking of such targets.

7. References

1. Otero M, Deresh B, Teig L, Werth J, Darrah C, Hsu K, Jones D, Holder J, Cagle R. RCS modeling of projectiles for counterfire radar performance simulations. MITRE Corporation (US); July 2007. Technical report.
2. FEKO EM Simulation Software Web page [accessed October 2014]. http://www.feko.info.
3. Dogaru T. AFDTD user's manual. Adelphi (MD): Army Research Laboratory (US); March 2010. Report No.: ARL-TR-5145.
4. Taflove A, Hagness S. Computational electrodynamics: The finite-difference time-domain method. Norwood (MA): Artech; 2000.
5. ARL DSRC Web page [accessed August 2015]. http://www.arl.hpc.mil.
6. AFRL DSRC Web page [accessed August 2015]. http://www.afrl.hpc.mil.
7. Navy DSRC Web page [accessed August 2015]. http://www.navydsrc.hpc.mil.
8. Richards M, Scheer J, Holm W. Principles of modern radar. Raleigh: SciTech Publishing; 2010.
9. Hubral P, Tygel M. Analysis of the Rayleigh pulse. Geophysics. 1989;54:654–658.
10. Dogaru T. The AFDTDGRID mesh generation software user's manual. Adelphi (MD): Army Research Laboratory (US); October 2010. Report No.: ARL-TR-5380.
11. Peterson A, Ray S, Mittra R. Computational methods for electromagnetics. New York: IEEE Press; 1997.
12. Knott E, Shaeffer J, Tuley M. Radar cross section. Boston: Artech House; 1993.

List of Symbols, Abbreviations, and Acronyms

ARL	US Army Research Laboratory
CAD	computer aided design
CPU	central processing unit
DSRC	Defense Supercomputing Resource Center
EM	electromagnetic
FDTD	finite difference time domain
GPS	global positioning system
H-H	horizontal-horizontal
HPC	High Performance Computing
PC	personal computer
PEC	perfect electric conductor
RAM	rocket, artillery and mortar
RCS	radar cross section
SIE	surface integral equation
V-V	vertical-vertical

1 DEFENSE TECH INFO CTR
(PDF) ATTN DTIC OCA

2 US ARMY RSRCH LAB
(PDF) ATTN IMAL HRA MAIL & RECORDS MGMT
ATTN RDRL CIO LL TECHL LIB

1 GOVT PRNTG OFC
(PDF) ATTN A MALHOTRA

7 US ARMY RSRCH LAB
(PDF) ATTN RDRL SER U
A SULLIVAN
C KENYON
C LE
D LIAO
T DOGARU
ATTN RDRL SER M
A HEDDEN
D WIKNER

INTENTIONALLY LEFT BLANK.